Reema P. Vazirani,[1] Akanksha Verma,[2] L. Amanda Sadacca,[1] Melanie S. Buckman,[3]
Belen Picatoste,[1] Muheeb Beg,[1] Christopher Torsitano,[1] Joanne H. Bruno,[1]
Rajesh T. Patel,[1] Kotryna Simonyte,[4] Joao P. Camporez,[5] Gabriela Moreira,[5]
Domenick J. Falcone,[6] Domenico Accili,[7] Olivier Elemento,[2] Gerald I. Shulman,[6,8]
Barbara B. Kahn,[4] and Timothy E. McGraw[1,3]

Disruption of Adipose Rab10-Dependent Insulin Signaling Causes Hepatic Insulin Resistance

Insulin controls glucose uptake into adipose and muscle cells by regulating the amount of GLUT4 in the plasma membrane. The effect of insulin is to promote the translocation of intracellular GLUT4 to the plasma membrane. The small Rab GTPase, Rab10, is required for insulin-stimulated GLUT4 translocation in cultured 3T3-L1 adipocytes. Here we demonstrate that both insulin-stimulated glucose uptake and GLUT4 translocation to the plasma membrane are reduced by about half in adipocytes from adipose-specific Rab10 knockout (KO) mice. These data demonstrate that the full effect of insulin on adipose glucose uptake is the integrated effect of Rab10-dependent and Rab10-independent pathways, establishing a divergence in insulin signal transduction to the regulation of GLUT4 trafficking. In adipose-specific Rab10 KO female mice, the partial inhibition of stimulated glucose uptake in adipocytes induces insulin resistance independent of diet challenge. During euglycemic-hyperinsulinemic clamp, there is no suppression of hepatic glucose production despite normal insulin suppression of plasma free fatty acids. The impact of incomplete disruption of stimulated adipocyte GLUT4 translocation on whole-body glucose homeostasis is driven by a near complete failure of insulin to suppress hepatic glucose production rather than a significant inhibition in muscle glucose uptake. These data underscore the physiological significance
of the precise control of insulin-regulated trafficking in adipocytes.

Insulin regulation of the amount of the GLUT4 in the plasma membrane of muscle and adipose cells has a major role in the control of postprandial blood glucose levels. In the basal (unstimulated) state, GLUT4 is retained intracellularly through rapid endocytosis and slow recycling back to the plasma membrane. The exclusion of GLUT4 from the plasma membrane limits basal glucose flux into fat and muscle cells. Insulin stimulation alters the kinetics of GLUT4 trafficking by accelerating exocytosis and slowing endocytosis, inducing a net redistribution of GLUT4 to the plasma membrane (1–3). The accumulation of GLUT4 in the plasma membrane results in increased glucose flux into cells and the postprandial disposal of glucose. The effect of insulin on glucose uptake into muscle and adipose can be accounted for by altered GLUT4 localization (4,5). Studies of genetically modified mice have established that the role of GLUT4 in insulin-stimulated glucose uptake into muscle (6) and adipose (7) are essential for the maintenance of glucose homeostasis. Furthermore, defective GLUT4 translocation is a hallmark of insulin resistance and type 2 diabetes in humans (8–10). Consequently, to fully understand insulin action and its disruption in metabolic disease,

[1]Department of Biochemistry, Weill Cornell Medical College, New York, NY
[2]Department of Physiology and Biophysics, Weill Cornell Medical College, New York, NY
[3]Department of Cardiothoracic Surgery, Weill Cornell Medical College, New York, NY
[4]Beth Israel Deaconess Medical Center, Harvard Medical School, Boston, MA
[5]Departments of Internal Medicine and Cellular & Molecular Physiology, Yale School of Medicine, Yale University, New Haven, CT
[6]Department of Pathology, Weill Cornell Medical College, New York, NY
[7]Department of Medicine and Naomi Berrie Diabetes Center, Columbia University, New York, NY
[8]Howard Hughes Medical Institute, Yale University, New Haven, CT

METABOLISM

it is essential to describe how the insulin signal is transduced to the regulation of GLUT4 trafficking at the molecular level.

Studies of the cultured 3T3-L1 adipocyte cell line have established that the AS160-Rab10 signaling module is essential for stimulated GLUT4 translocation to the plasma membrane (11–15). Insulin activation of the Akt serine-threonine protein kinase leads to the phosphorylation and inactivation of the AS160 (TBC1D4) Rab GTPase activating protein (16). Although AS160 has activity toward a number of Rab proteins (17), Rab10 is the AS160 target Rab involved in the regulation of GLUT4 trafficking in cultured adipocytes. In cultured muscle cells, Rab8a, but not Rab10, mediates GLUT4 trafficking. In unstimulated 3T3-L1 adipocytes, the GTPase activity of AS160 maintains Rab10 in the inactive guanosine diphosphate–bound state. Insulin-stimulated inactivation of AS160 leads to the Rab10-dependent translocation of GLUT4 to the plasma membrane (11). Rab10 knockdown with small interfering RNA (siRNA) reduces insulin-stimulated GLUT4 translocation by about half in 3T3-L1 adipocytes, suggesting that multiple signaling pathways downstream of the insulin receptor are required for the stimulation of GLUT4 translocation (13). It is unknown whether there are both Rab10-dependent and Rab10-independent pathways in primary adipocytes. This phenomenon described in studies of cultured cells could be a consequence of incomplete Rab10 depletion by siRNA knockdown, which would allow residual Rab10 activity, or it could be a characteristic of the cultured 3T3-L1 adipocyte line. Knowing how the insulin signal is transduced to GLUT4 in vivo is key for understanding the physiological activity of insulin and its disruption in disease.

We created adipose-specific Rab10 knockout (KO) mice to evaluate the contribution of Rab10 to insulin regulation of GLUT4 trafficking in primary adipocytes. These studies demonstrate that Rab10 is an essential component of the machinery responsible for insulin stimulation of GLUT4 trafficking to the plasma membrane of primary adipocytes. Approximately half of the insulin signal to GLUT4 requires Rab10, establishing that the full effect of insulin on GLUT4 requires both Rab10-dependent and Rab10-independent pathways. Adipose-specific Rab10 KO mice on a normal chow diet are insulin intolerant, and during euglycemic-hyperinsulinemic clamp they have severely blunted inhibition of hepatic glucose production. The demonstration that a partial defect in adipocyte GLUT4 translocation can induce insulin resistance establishes the importance of fully intact insulin regulation of adipocyte glucose transport in glucose homeostasis.

RESEARCH DESIGN AND METHODS

AR10KO Mice
Embryonic stem cells containing a Rab10 conditional KO construct (Knockout Mouse Project CSD44891) were microinjected to generate chimera mice. Offspring with the construct were crossed with Flipase transgenic mice to remove the selection cassette and generate carriers of a conditional Rab10 allele containing loxP sites flanking exon 1 of Rab10. The colony was backcrossed to C57BL/6J mice four times. Heterozygotes with (Rab10$^{fl/wt}$ + cre) and without (Rab10$^{fl/wt}$) the adiponectin-cre transgene were bred to generate mice for the majority of experiments. Homozygote flox females (Rab10$^{fl/fl}$) and AR10KO males (Rab10$^{fl/fl}$ + cre) were bred to generate mice for the euglycemic-hyperinsulinemic clamp. Control data were derived from littermate controls. The metabolic phenotypes of wild-type, cre, and flox (Rab10$^{fl/fl}$) mice did not vary while eating a low-fat diet (LFD) (Supplementary Figs. 2 and 3). Mice were maintained on a standard 12-h light/dark cycle, and had ad libitum access to water and food. Mice were fed standard rodent chow except where noted that mice were fed a high-fat diet (HFD) or LFD (catalog #D12492 or #D12450B; Research Diets). Unless otherwise noted, all experiments were performed using female mice. All protocols were approved by the Weill Cornell Medical College and Yale Medical School Institutional Animal Care and Use Committees.

Genotyping
Tail DNA retrieved through proteinase K digestion was used in touchdown PCR (at 65–55°C, followed by 30 cycles at 94°C for 30 min, at 55°C for 30 min, and at 72°C for 60 min) with the following primer pairs: Rab10 (5′-GGTAAAGG CAAGTAGATGTCCATG-3′, 5′-GAAGAGCAATTAAACACTG CATGC-3′) and Cre Recombinase (5′-ATGTCCAATTTACTG ACCG-3′, 5′-CGCCGCATAACCAGTGAAAC-3′).

Tissue Immunoblotting
Tissues were processed using a multisample pulverizer and were prepared in lysis buffer (catalog #9803S; Cell Signaling Technology) containing HALT inhibitor cocktail (catalog #78442; Thermo Scientific). An equivalent amount of protein was used for all samples in each gel. Membranes were incubated with primary antibodies at 4°C overnight, as follows: Rab10 (1:500; catalog #4262; Cell Signaling Technology), GLUT4 (1:25,000; catalog #2213; Cell Signaling Technology), phosphorylated AS160 T642 (1:1,000; catalog #8881; Cell Signaling Technology), AS160 (1:5,000; catalog #07–741; Millipore), Rab8a (1:1,000; catalog #610844; BD Biosciences), phosphorylated Akt S473 (1:2,000; catalog #9271; Cell Signaling Technology), and Akt (1:1,000; catalog #9272; Cell Signaling Technology).

Adipocyte Glucose Uptake and Size Measurement
Primary adipocyte glucose uptake and size measurement was performed as previously described (7), except for the use of tracer amounts of ^{3}H-2-deoxyglucose (50 nmol/L; catalog #NET549250UC; PerkinElmer) diluted in 5 μmol/L glucose. Glucose uptake using a higher concentration of 2-deoxyglucose has been shown to be linear for up to 30 min in primary adipocytes (18). Briefly, dissociated adipocytes from female mice were treated with insulin for 20 min prior to the addition of ^{3}H-2-deoxyglucose. After 20 min of uptake, cells were collected for scintillation

counting. An aliquot of the cell suspension was osmium fixed and used to normalize results as well as to measure cell diameter.

GLUT4 Translocation in Stromal Vascular Fraction Adipocytes

The stromal vascular fraction (SVF) was isolated from digested subcutaneous fat pads and cultured in DMEM/F12 media containing 15% FBS. Cells were infected with lentiviral particles carrying the pLenti6/V5-D-TOPO hemagglutinin (HA)-GLUT4-GFP expression construct prior to differentiation. Upon confluence, cells were differentiated in DMEM/F12 media containing 10% FBS, 1 μmol/L rosiglitazone, 0.25 μmol/L dexamethasone, 0.5 mmol/L 3-isobutyl-1-methylxanthine, and 1 μg/mL insulin (day 0). After 2 days, SVF adipocytes were maintained in media containing 10% FBS and insulin. Insulin was removed at least 24 h before the assay. Briefly, cells were serum starved for 2 h, insulin was applied for 30 min, and anti-HA antibody (1:1,000; catalog #MMS-101; BioLegend) was used to detect GLUT4 on the cell surface. The surface HA signal was normalized to the GFP signal to account for the amount of HA-GLUT4-GFP reporter in the cell. The expression of adipocyte differentiation markers was assessed using adiponectin (Acrp30, 1:300; catalog #26497; Santa Cruz Biotechnology) and perilipin (1:300; catalog #9349; Cell Signaling Technology) primary antibodies.

Glucose and Insulin Tolerance Tests

For glucose tolerance tests (GTTs), 4- to 5-month-old mice were fasted overnight prior to 2 g/kg i.p. injection of glucose. For insulin tolerance tests (ITTs), 4- to 5-month-old mice were fasted 4 h prior to intraperitoneal injection of 0.75 or 1 unit/kg insulin for LFD- or HFD-fed mice, respectively. Tail blood glucose was measured at various time points after injections.

Plasma Measurements

Plasma insulin (Mouse Ultrasensitive Insulin ELISA; Cayman Chemical), glycerol (MAK117; Sigma-Aldrich), and nonesterified fatty acids (NEFAs) (HR series; Wako) were measured following manufacturer instructions. Diluted plasma (1:30, 45 μL/lane) was immunoblotted for retinol-binding protein (RBP) (1:1,000; catalog #A0040; Dako). For each blot, quantification was normalized to the average of controls. Leptin and adiponectin were measured by the Biomarker and Analytic Research Core at the Einstein-Mount Sinai Diabetes Research Center (EZML, EZMADP; EMD Millipore).

Euglycemic-Hyperinsulinemic Clamps

Euglycemic-hyperinsulinemic clamps were performed by the Yale Mouse Metabolic Phenotyping Center as previously described (19). Briefly, 6-month-old female mice were infused with ^{3}H-glucose, and blood samples were collected at various time intervals. During the clamp, insulin was infused at a constant rate (2.5 mU/kg/min), while glucose was infused at a variable rate to target of 120 mg/dL. Scintillation counting of infusates and blood samples allowed for the calculation of glucose appearance and disposal.

RNA Preparation

Snap-frozen tissues were processed using a multisample pulverizer and liquid nitrogen followed by lysis in Qiazol (catalog #79306; Qiagen). RNA extraction was performed using the Lipid Tissue Mini Kit (catalog #74804; Qiagen) according to the manufacturer instructions.

RNA Sequencing Analysis

RNA-seq data from control and AR10KO sample sets were aligned to the mouse genome (mm10) using Spliced Transcripts Alignment to a Reference software (20). Aligned reads were quantified for gene counts and levels of fragments per kilobase of transcript per million mapped reads, using HTSeq-count (21) and CuffLinks (22), respectively. Initial sample clustering revealed a batch effect for samples processed with different RNA extraction kits on different dates. A two-factor analysis design using the Limma (23) package in R statistical software was used for the correction of batch effects and differential expression analysis based on gene counts. Gene signatures were curated using the top 50 most significantly upregulated genes. Using Gene Set Enrichment Analysis software (24), gene ontology was performed using the GLUT4 KO gene signature against the Rab10 KO data set and also using the Rab10 KO signature against the adipose GLUT4 KO data set.

RESULTS

Adipose Rab10 KO Mice

Cre-lox recombination was used to generate adipose-specific Rab10 KO (AR10KO) mice. Mice with loxP sites flanking exon 1 of Rab10 were bred with adiponectin-cre transgenic mice (25) to specifically drive deletion of Rab10 in mature adipocytes. AR10KO mice were generated at the expected Mendelian frequency ($P > 0.99$), and, unlike whole-body Rab10 KO (26), adipose-specific KO was not embryonically lethal. In AR10KO mice, Rab10 protein expression was lost in white and brown adipose tissues, while remaining unchanged in liver and skeletal muscle (Fig. 1A). Rab10 expression did not vary among control genotypes (Supplementary Fig. 1). Immunohistochemistry of visceral white adipose tissue (WAT) did not reveal gross morphological changes in AR10KO WAT (Fig. 1B). Lipid droplet size was also unchanged (data not shown). Furthermore, there was no change in adipocyte size in freshly dissociated perigonadal adipocytes from the AR10KO mice (Fig. 1C). To query whether Rab10 KO disrupts the expression of other proteins known to have a role in the regulation of GLUT4 trafficking, immunoblots were performed on perigonadal WAT lysates. The expression of GLUT4 (a functional target of Rab10) and AS160 (a Rab10 regulator) were not changed in AR10KO WAT (Fig. 1D). The expression of Rab8a, which is required for GLUT4 translocation in cultured muscle cells (27) but not in cultured adipocytes (13), was unchanged in AR10KO WAT (Fig. 1D), demonstrating that the expression of Rab8a is not altered in compensation for Rab10 deletion.
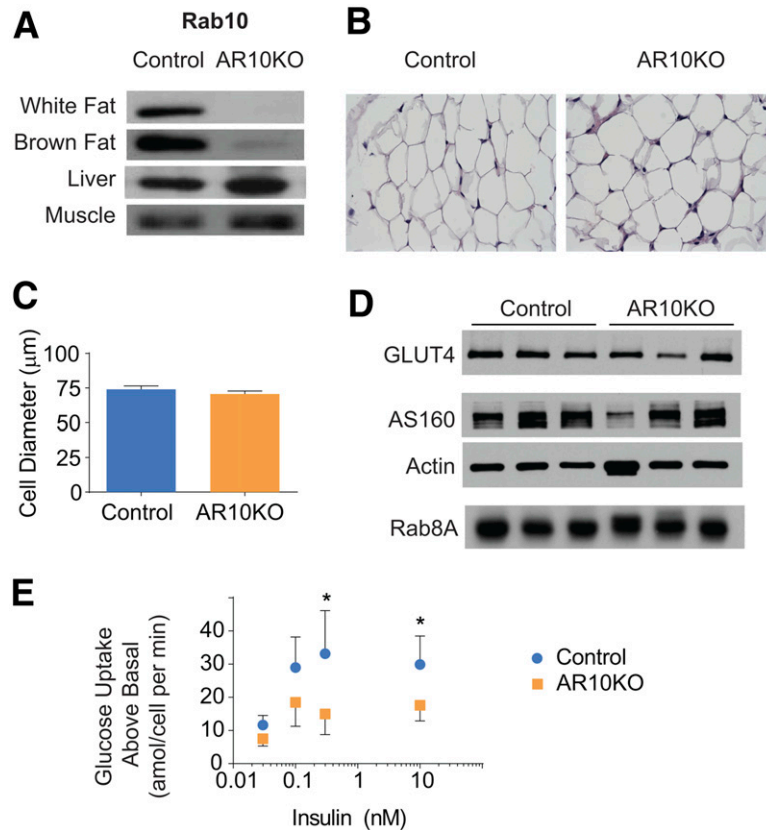
Figure 1—Adipose Rab10 deletion impairs insulin-stimulated glucose uptake in primary adipocytes. *A*: Rab10 representative immunoblots of tissue extracts from control and AR10KO mice. *n* > 5. *B*: Representative hematoxylin-eosin staining of fixed perigonadal adipose tissue sections. *n* > 5. *C*: Primary adipocyte cell diameter. *n* > 7 mice, >40 cells. *D*: Representative perigonadal adipose tissue immunoblots for GLUT4, AS160, actin, and Rab8a. *n* > 5. *E*: Insulin-stimulated glucose uptake above basal in adipocytes freshly dissociated from perigonadal WAT of female mice. *n* > 7. *P < 0.05.

Rab10 Deletion Blunts Insulin-Stimulated Glucose Uptake in Freshly Dissociated Adipocytes

Insulin stimulated glucose uptake in primary adipocytes acutely isolated from perigonadal WAT (Fig. 1*E*). Rab10 deletion resulted in a 50% reduction of insulin-stimulated glucose uptake, demonstrating that Rab10 is required for insulin action in freshly dissociated mouse adipocytes.

Insulin-Stimulated GLUT4 Redistribution to the Cell Surface Is Reduced in Adipocytes From Adipose Rab10 KO Mice

To determine the effect of Rab10 KO on insulin-regulated GLUT4 trafficking, the behavior of the dual-tagged GLUT4 reporter HA-GLUT4-GFP (28,29) was studied in AR10KO adipocytes. This construct has an HA epitope inserted in the first exofacial loop, and GFP fused to the carboxyl cytoplasmic domain of GLUT4. HA-GLUT4-GFP in the plasma membrane can be quantified by indirect immunofluorescence of the exofacial HA tag in fluorescence microscopy of nonpermeabilized adipocytes. The ratio of the anti-HA fluorescence (surface) to GFP fluorescence (total) reflects the fraction of GLUT4 in the plasma membrane per cell.

The cellular distribution of HA-GLUT4-GFP was evaluated in adipocytes differentiated in vitro from the subcutaneous adipose SVF. We first studied the behavior of HA-GLUT4-GFP expressed by the electroporation of adipocytes at day 6 of in vitro differentiation. We have previously shown (30) that after electroporation we cannot use lipid droplets to reliably identify adipocytes. Therefore, we confirmed that electroporated SVF cells at day 6 of in vitro differentiation were adipocytes by staining for perilipin (31) or adiponectin (32) (Fig. 2*A*). Insulin stimulates GLUT4 translocation to the cell surface in electroporated perilipin-expressing SVF day 6 adipocytes (Fig. 2*B*). Quantification of GLUT4 distribution revealed a significant, although partial, blunting (~30% reduction) of insulin-stimulated translocation in AR10KO SVF adipocytes expressing perilipin (Fig. 2*C*).

To investigate the effect of Rab10 KO at a later stage of differentiation (day 8) and without the potential effects of electroporation, lentiviral infection was used to drive the expression of HA-GLUT4-GFP. A comparable defect in insulin-mediated GLUT4 translocation to the cell surface (~50% reduction) was observed at this later stage of differentiation in lipid-droplet containing SVF adipocytes (Fig. 2*D* and *E*), confirming that Rab10 deletion causes a
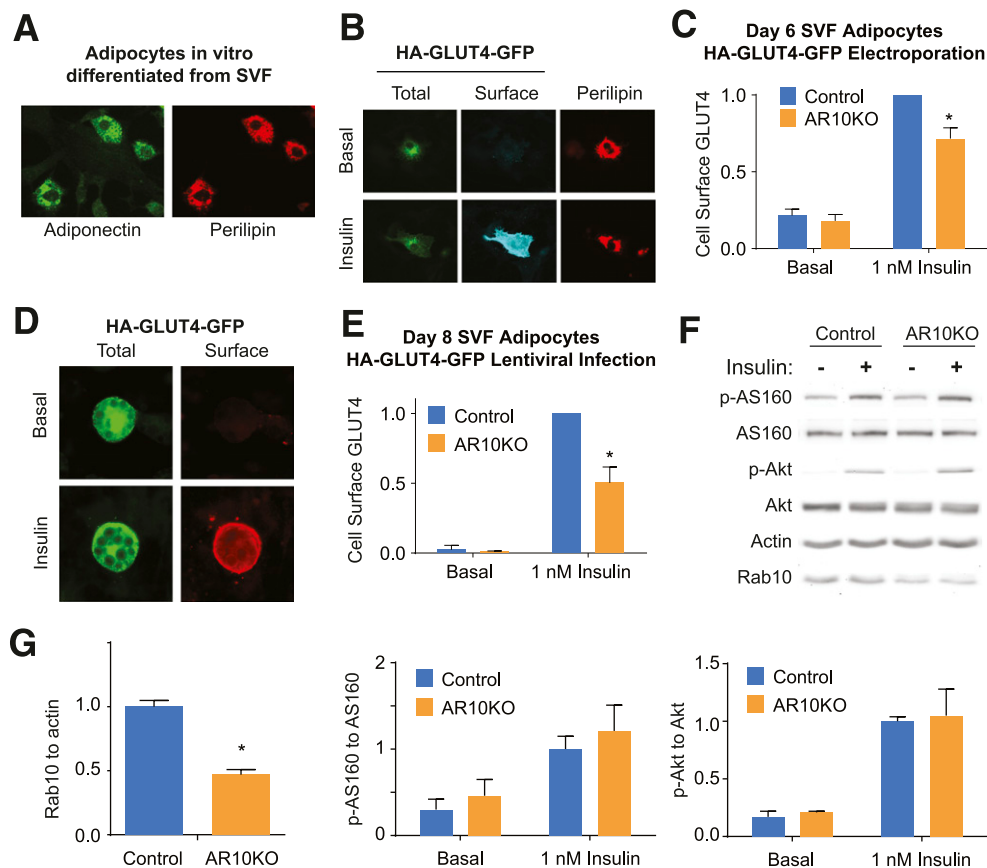
Figure 2—GLUT4 translocation to the cell surface in response to insulin is blunted in AR10KO SVF adipocytes. *A*: Immunofluorescence staining for adiponectin and perilipin in day 6 electroporated SVF adipocytes. *B* and *D*: Immunofluorescence staining of basal and 1 nmol/L insulin-treated SVF adipocytes expressing the reporter HA-GLUT4-GFP. Staining for extracellular HA in nonpermeablized cells shows HA-GLUT4-GFP at the surface in insulin-treated cells (Surface). GFP signal shows total HA-GLUT4-GFP (Total). Reporter expression was induced by electroporation (*B*) or lentiviral infection (*D*). *C* and *E*: Quantification of the surface-to-total ratio of HA-GLUT4-GFP in perilipin-expressing day 6 SVF adipocytes ($n = 4$ experiments, >20 cells) (*C*) and in lipid droplet–containing day 8 SVF adipocytes ($n = 4$ experiments, >30 cells) (*E*). *F* and *G*: Immunoblots and quantification of basal or 1 nmol/L insulin-treated SVF culture extracts for phosphorylated (p) Akt (S473), total Akt, phosphorylated AS160 (T642), total AS160, actin, and Rab10 ($n = 4$). *$P < 0.05$.

partial inhibition of insulin-stimulated GLUT4 translocation to the plasma membrane of adipocytes.

Insulin stimulation of AS160 phosphorylation (T642) and Akt phosphorylation (S473) were not reduced in cultured AR10KO SVF cells containing a mixture of undifferentiated cells and differentiated adipocytes (Fig. 2*F* and *G*). Rab10 expression is reduced by 60%, corresponding to the proportion of cells that differentiated into adipocytes. The background level of Rab10 expression seen is likely due to the presence of undifferentiated cells. Because AS160 expression is strongly induced by adipocyte differentiation by approximately sixfold to eightfold (33,34), AS160 expression and its phosphorylation more specifically reflect insulin signaling of the differentiated adipocytes within the population. This suggests that insulin signal transduction is not altered in AR10KO SVF adipocytes. Thus, the defect in insulin action in AR10KO SVF adipocytes is due to the loss of Rab10 regulation of GLUT4 trafficking. These data demonstrate that the function of Rab10 in insulin-stimulated

GLUT4 translocation, previously described in cultured 3T3-L1 adipocytes, translates to primary murine adipocytes.

Adipose Rab10 KO Mice Are Insulin Resistant

The deletion of Rab10 from adipose did not significantly change the ad libitum body weight of female mice being fed an LFD or HFD up to 20 weeks of age (Fig. 3*A*) or body weight after a 4-h fast at 18 weeks of age (data not shown) compared with their diet controls. Overall body composition is the same in chow-fed mice (Fig. 3*B*). Fasting blood glucose and plasma insulin levels were also unchanged (Table 1). However, as expected, HFD induced both weight gain and elevated fasting blood glucose concentrations. Although GTT results did not show significant changes between controls and AR10KO mice being fed each diet (Fig. 3*C*–*E*), ITT results revealed that AR10KO mice are insulin resistant while being fed both an LFD and an HFD (Fig. 3*F*–*I*). As a result of HFD-induced insulin resistance, a higher dosage of insulin was required to observe the further increase in insulin
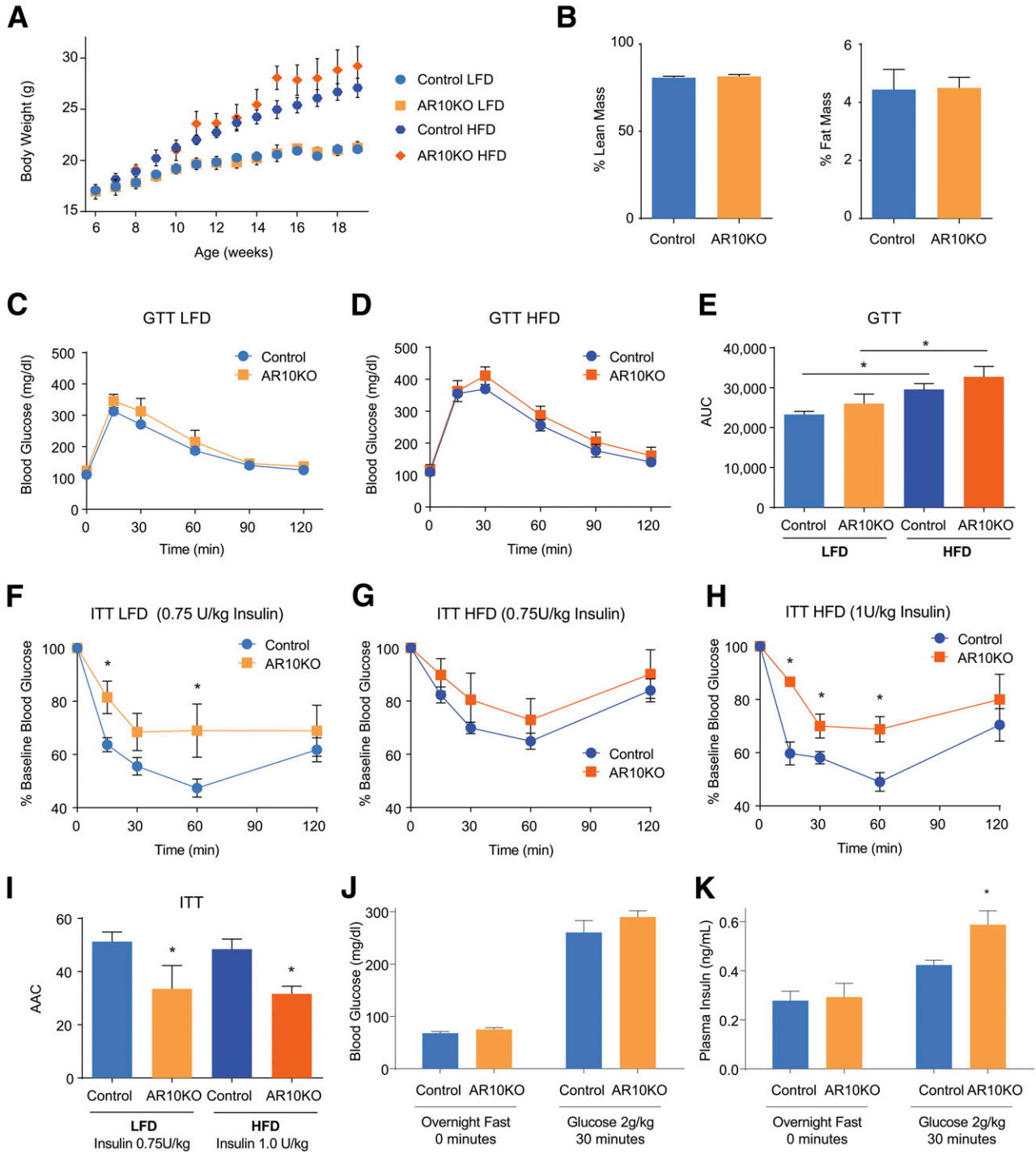
Figure 3—AR10KO mice are insulin resistant. *A*: Body weight (ad libitum) of female mice put on LFD or HFD at 6 weeks of age. *B*: Body composition of chow-fed female mice. *n* > 5. *C* and *D*: GTTs (2 g/kg glucose i.p.) of female mice being fed an LFD (*C*) or an HFD (*D*). *n* > 6. *E*: Quantification of GTT area under the curve (AUC). *F* and *G*: ITT results for female mice being fed an LFD (0.75 units/kg insulin i.p.) (*F*) or an HFD (0.75–1 unit/kg insulin i.p.) (*G* and *H*). *n* > 6. *I*: Quantification of ITT area above the curve (AAC). Blood glucose (*J*) and plasma insulin (*K*) levels in chow-fed female mice after overnight fasting and 30 min after intraperitoneal glucose injection (2 g/kg). *n* > 8. *P < 0.05.

intolerance in AR10KO mice being fed an HFD (Fig. 3*H*). Of note, we found that the adiponectin-cre mice displayed a degree of protection against HFD-induced glucose intolerance and fasting glucose elevation (Supplementary Fig. 2); therefore, adiponectin-cre mice were not included in the HFD control group.

The finding of glucose tolerance in the context of insulin resistance suggests compensation with increased

Table 1—Measurements in blood (glucose) or plasma (insulin, adiponectin, leptin, glycerol, NEFA, RBP) after overnight fasting of 23-week-old female mice

	Diet	Control	AR10KO
Glucose (mg/dL)	LFD	79.0 ± 4.4	84.3 ± 6.0
Insulin (ng/mL)	LFD	0.38 ± 0.07	0.35 ± 0.05
Glucose (mg/dL)	HFD	92.3 ± 4.5	98.4 ± 6.4
Insulin (ng/mL)	HFD	0.34 ± 0.10	0.36 ± 0.06
Adiponectin (μg/mL)	LFD	26.2 ± 3.8	23.0 ± 3.4
Leptin (ng/mL)	LFD	3.5 ± 0.9	4.0 ± 1.1
Glycerol (mmol/L)	LFD	0.40 ± 0.02	0.40 ± 0.03
NEFA (mEq/L)	LFD	0.72 ± 0.11	0.69 ± 0.09
RBP (arbitrary units)	LFD	1.00 ± 0.15	1.22 ± 0.20

Data reported as the average ± SEM. n = 6–9/group.

insulin secretion. Blood glucose and plasma insulin were measured after overnight fasting and 30 min after intraperitoneal injection of glucose. Because insulin resistance was observed in mice being fed an LFD, these studies were performed in chow-fed mice. As seen in mice being fed an LFD, fasting blood glucose and plasma insulin concentrations were unchanged (Fig. 3*J* and *K*). However, 30 min after intraperitoneal injection of glucose, the blood glucose concentrations of AR10KO mice were the same as those of controls (Fig. 3*J*), while plasma insulin levels of AR10KO mice were 40% higher than those in controls (Fig. 3*K*). These data show that insulin secretion is increased to compensate for insulin resistance, resulting in normal glucose tolerance.

The circulating levels of leptin, adiponectin, and RBP, three adipokines involved in the control of whole-body insulin sensitivity (35–37), were not significantly changed in AR10KO mice (Table 1). In addition, fasting plasma glycerol and NEFA levels were unchanged, suggesting that increased adipocyte lipolysis does not underlie the insulin resistance (Table 1).

Adipose Rab10 KO Insulin Resistance Is Mediated by Loss of Hepatic Insulin Sensitivity

Euglycemic-hyperinsulinemic clamps were performed to characterize the insulin resistance in female AR10KO mice. The glucose infusion rate required to maintain euglycemia during the infusion of 2.5 mU/kg · min insulin was 30% lower in AR10KO mice (Fig. 4*A* and *B*). Whole-body insulin-stimulated glucose uptake displayed a trend for a 10% reduction in AR10KO mice (Fig. 4*C*). Although there was a trend for a small decrease in insulin-stimulated 2-deoxyglucose uptake in AR10KO muscle (Fig. 4*D*), uptake was significantly reduced in WAT (Fig. 4*E*). The magnitude of the WAT 2-deoxyglucose uptake defect is ~50%, which is similar to the defect in glucose uptake observed in dissociated adipocytes. Insulin suppression of hepatic glucose production was almost completely lost in AR10KO mice, showing that the decrease in glucose infusion rate is primarily mediated by hepatic

insulin resistance (Fig. 4*F*). Interestingly, insulin-mediated suppression of plasma free fatty acids is maintained (Fig. 4*G*), showing that adipose insulin sensitivity is also maintained. Together, these data demonstrate a striking hepatic insulin resistance driven by Rab10 deletion in adipocytes, independent of adipose insulin sensitivity.

Adipose Rab10 and GLUT4 KO Models Display Similar Changes in the WAT Transcriptome, Showing That Reduced Adipocyte Glucose Uptake Mediates AR10KO Insulin Resistance

To better understand the role of adipose Rab10 in systemic insulin sensitivity, we turned to the adipose-specific GLUT4 KO model in which insulin-stimulated glucose transport into adipocytes is lost, resulting in whole-body insulin resistance (7). In the adipose GLUT4 KO model, the changes in adipocyte biology are necessarily downstream of reduced glucose uptake. The loss of insulin-stimulated glucose uptake in the adipose-specific GLUT4 KO is linked to transcriptional alterations (38) that contribute to the systemic insulin resistance. In vivo genetic manipulation of the genes associated with altered transcripts shows that several could contribute to the insulin-resistant phenotype induced by adipose GLUT4 KO, suggesting that cumulative transcriptional changes may underlie the mechanism (37–40).

To determine whether similar changes occur in the AR10KO WAT, RNA sequencing was performed on perigonadal WAT RNA from three AR10KO mice and three control mice. The gene expression data clustered by genotype, demonstrating a distinct transcriptional profile of AR10KO perigonadal WAT (Fig. 5*A*). We next generated gene expression profiles of the WAT from adipose GLUT4 KO mice (38) (Gene Expression Omnibus accession #GSE35378) and AR10KO mice (Gene Expression Omnibus accession #GSE70123) (Supplementary Table 1) composed of the top 50 upregulated genes for each model. We then used these profiles in gene set enrichment analyses to explore potential similarities in upregulated genes between AR10KO and adipose-GLUT4 KO. The set of genes upregulated in AR10KO WAT is significantly upregulated in adipose GLUT4 KO WAT ($P < 0.001$) (Fig. 5*B*), and, likewise, the gene set upregulated in adipose GLUT4 KO WAT is significantly upregulated in AR10KO WAT ($P < 0.005$) (Fig. 5*C*). These data demonstrate common transcriptome changes in AR10KO and the adipose GLUT4 KO mice, which is inconsistent with the possibility that the perturbation of a different Rab10-dependent activity in adipocytes mediates the AR10KO phenotype. This finding is particularly significant because Rab10 KO would affect trafficking of other components and proteins in the vesicles carrying GLUT4 (41), whereas GLUT4 KO would not. Furthermore, the function of Rab10 may not be restricted to insulin-regulated trafficking. Rab10 has been shown in other cell types to function in different membrane trafficking pathways (42–45). However, because GLUT4 KO would not alter these pathways, the fact that the set of
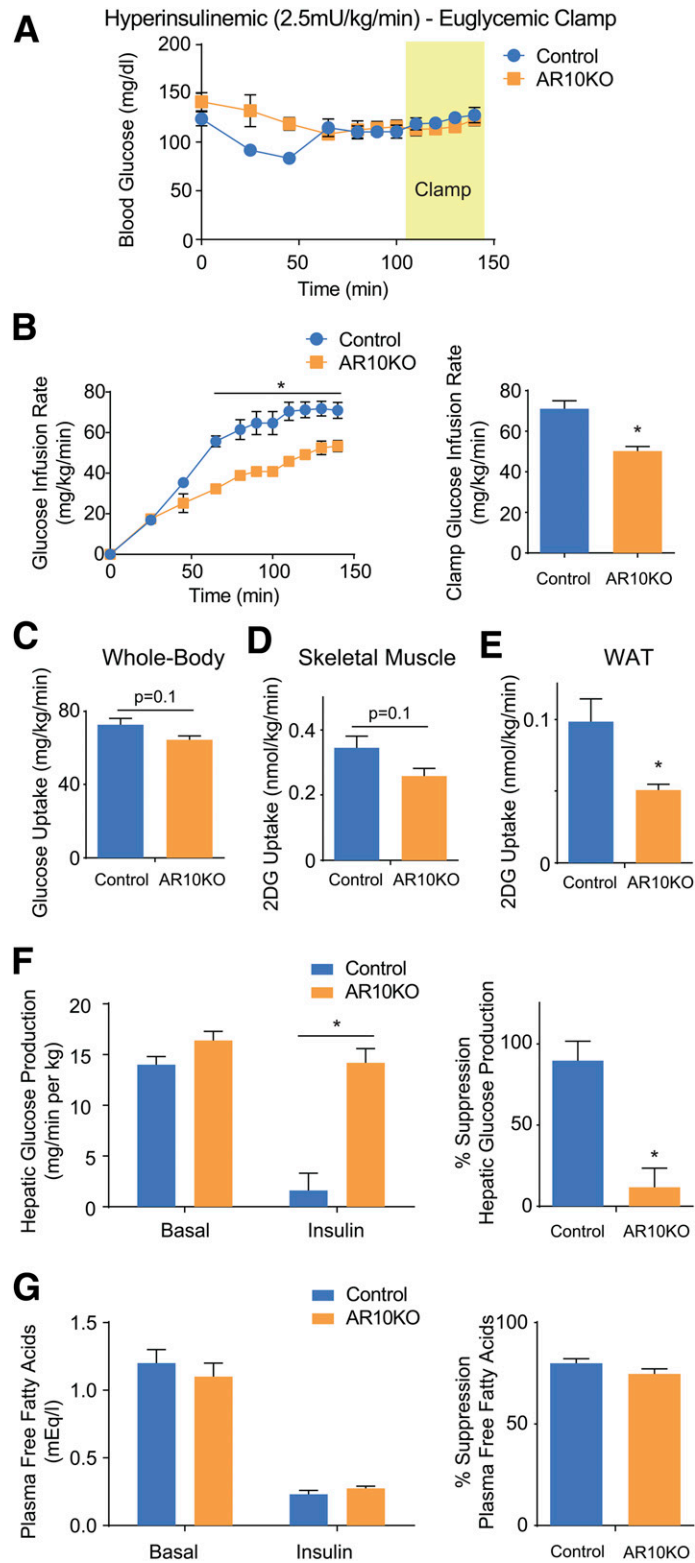
Figure 4—Euglycemic-hyperinsulinemic clamp of female mice. *A*: Blood glucose levels. *B*: Glucose infusion rate required to maintain euglycemia. Whole-body glucose uptake (*C*) and gastrocnemius skeletal muscle (*D*) and WAT (*E*) 2-deoxyglucose (2DG) uptake during clamp. *F*: Hepatic glucose production and suppression. *G*: Plasma free fatty acid concentration and suppression. $n > 5$. *$P < 0.05$.

A

B

C

D
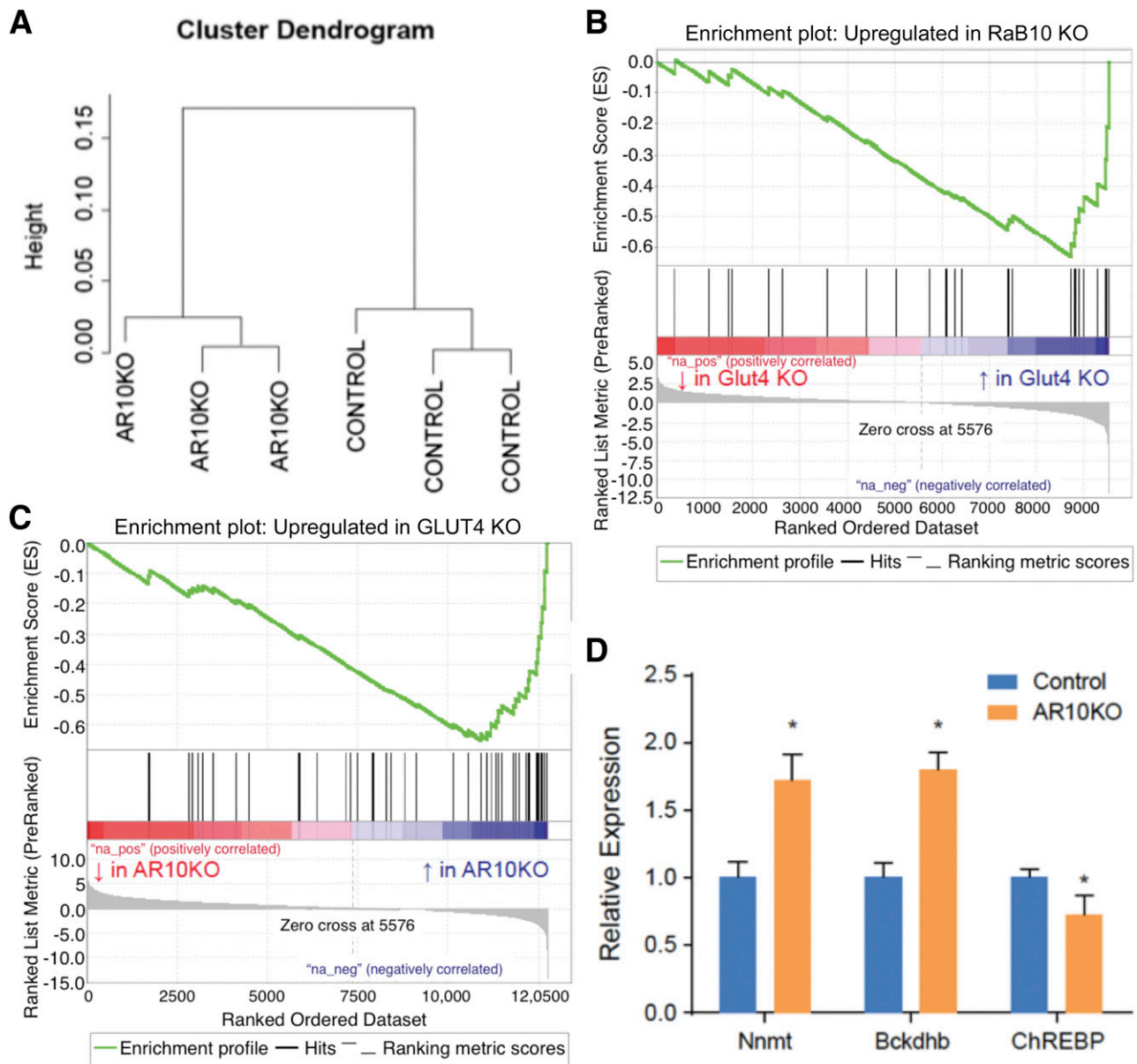
Figure 5—RNA sequencing analysis reveals similar changes in AR10KO and adipose GLUT4 KO WAT transcriptomes from female mice. *A*: Data clustering. *B*: AR10KO WAT gene set enrichment in adipose GLUT4 KO WAT. *C*: Adipose GLUT4 KO WAT gene set enrichment in AR10KO WAT. *D*: RT-PCR of proposed mediators of adipose GLUT4 KO. $n = 8$. *$*P < 0.05$.

upregulated GLUT4 KO WAT genes is significantly upregulated in AR10KO WAT supports the conclusion that metabolic dysregulation of the AR10KO mouse is specifically downstream of reduced insulin-stimulated glucose uptake into the Rab10 KO adipocytes.

The proposed mediators of the adipose GLUT4 KO phenotype include increased RBP4 (37), increased branched-chain amino acid enzymes (39), decreased carbohydrate response element–binding protein (ChREBP) (38), and increased nicotinamide N-methyltransferase (Nnmt) (40). RT-PCR from Rab10 KO WAT RNA show increased branched-chain ketoacid dehydrogenase E1 β (Bckdhb), decreased total ChREBP (Mlxipl), and increased Nnmt

(Fig. 5D). These data support the likelihood that similar mediators, downstream of reduced insulin-stimulated glucose flux into adipocytes, cumulatively cause insulin intolerance in both the adipose GLUT4 KO and the AR10KO mice.

DISCUSSION

Regulation of GLUT4 trafficking is a major activity of insulin action in adipose. Studies in 3T3-L1 cells as an in vitro model of adipocytes have led to the identification of a number of components of the insulin-regulated GLUT4 trafficking machinery, most prominently the AS160-Rab10 module (11–13). Although there are extensive data linking

Rab10 to insulin control of GLUT4 in the 3T3-L1 cultured adipocyte cell line, the role of Rab10 in in vivo adipocyte biology had not been investigated. The AR10KO model demonstrates in vivo that Rab10 is a key effector for insulin signaling in adipose and that Rab10 function in adipose is essential for systemic metabolic regulation.

The role of AS160 has been probed in genetic mouse models using conventional whole-body deletion of AS160. Two separate AS160 KO mouse models were found to be insulin resistant (46,47). Characterization of glucose uptake and GLUT4 trafficking in adipose and muscle tissues showed that only adipocyte basal glucose uptake was increased, whereas insulin-stimulated glucose uptake and GLUT4 trafficking were impaired in both adipocytes and soleus muscle. Because AS160 is active in the absence of insulin signaling, these models would have been expected to largely reflect the loss of GLUT4 retention in the basal state. However, the findings also showed dysregulation in the insulin state. Because AS160 is important for both muscle and adipose GLUT4 trafficking, these models are unable to address tissue-specific contributions. Additionally, AS160 has alternate roles in the heart (48) and renal epithelial cells (49), which would have also been affected. Hence, our AR10KO model was designed to be tissue specific and to probe not only the relevance of Rab10, but also of glucose uptake, specifically in the insulin stimulated state.

Despite the shared requirement for AS160 in insulin regulation of glucose transport into muscle and adipose, studies of cultured cells suggest that Rab8a, but not Rab10, functions downstream of AS160 in muscle (27), whereas Rab8a does not have a role in GLUT4 trafficking in 3T3-L1 adipocytes (13). This tissue-specific AS160 substrate Rab protein requirement for GLUT4 translocation was unexpected, calling into question whether the distinct Rab protein requirements in cultured cells was indicative of the machinery requirements in primary cells. Here we unequivocally establish a role for Rab10 in insulin-stimulated glucose uptake by primary adipocytes.

Past studies (11,13) using siRNA knockdown strategies in cultured adipocytes have shown that about half of the impact of insulin signaling on GLUT4 translocation in 3T3-L1 adipocytes is transmitted via AS160-Rab10. However, until this report it was not known whether the partial effect was the true contribution of Rab10, whether it was due to incomplete Rab10 knockdown by siRNA or whether it was a phenomenon that was limited to the cultured cell model. The fact that Rab10 KO partially inhibits insulin-stimulated glucose uptake by primary adipocytes and partially blunts GLUT4 translocation has important ramifications for understanding insulin control of glucose transport in adipocytes. These data establish that Rab10-dependent and Rab10-independent signaling downstream of the insulin receptor are required in vivo for the full effect of insulin on GLUT4 translocation. Thus, a complete description of insulin control of GLUT4 requires the identification of both the Rab10-dependent and Rab10-independent pathways. It is likely

that the signaling diverges downstream of Akt because direct activation of Akt induces full GLUT4 translocation (50). The Rab10-independent pathway may be independent of AS160 as well, because insulin promotes a redistribution of GLUT4 in AS160 KO and knockdown adipocytes, revealing AS160-independent control of GLUT4 trafficking (11,46). A number of potential Rab10-independent pathways downstream of the insulin receptor in 3T3-L1 adipocytes involved in GLUT4 translocation have been reported, including the Rab3-Noc2 module (51) and TUG (52), although how these integrate with Rab10 signaling are not known.

Studies of cultured 3T3-L1 adipocytes (29,30) have identified insulin stimulation of GLUT4 vesicle formation, docking to the plasma membrane, and fusion with the plasma membrane as potential sites of insulin regulation of exocytosis. The requirement of Rab10-dependent and Rab10-independent signaling for the full effect of insulin suggests that these pathways regulate different steps of GLUT4 exocytosis and that an increased plasma membrane GLUT4 level is the summation of these effects. Previous studies (13) have shown that Rab10 regulates GLUT4 vesicle exocytosis prior to vesicle docking/fusion with the plasma membrane. A consequence of the regulation of multiple sequential steps is an amplification of the insulin effect and a more precise control of the amount of GLUT4 in the plasma membrane than could be achieved by the regulation of a single step.

Possible insulin resistance had the potential to confound the interpretation of the impairment of glucose uptake in freshly dissociated adipocytes from AR10KO mice. However, analyses of GLUT4 translocation in Rab10 KO SVF adipocytes (as opposed to freshly dissociated adipocytes) demonstrate that the blunting of GLUT4 translocation is a direct effect of Rab10 on the trafficking of GLUT4 and is not secondary to changes in signaling because insulin signaling in AR10KO SVF adipocytes is intact. Therefore, these data establish that reduced glucose uptake into primary AR10KO adipocytes is due to a direct effect of Rab10 rather than being secondary to the whole-body insulin resistance of the AR10KO mice.

Adipocytes from insulin-resistant humans harbor cell-autonomous changes that impede insulin-stimulated GLUT4 translocation to the cell surface (8). The magnitude of this defect worsens as insulin sensitivity deteriorates, such that adipocytes from individuals with mild insulin resistance still have a GLUT4 translocation response to insulin, albeit to a reduced degree compared with that of adipocytes from insulin-sensitive people (8). The decreased insulin sensitivity induced by moderate impairment of GLUT4 translocation in the AR10KO mouse implicates the blunted GLUT4 translocation in individuals with mild insulin resistance as a contributing factor in the progression to more pronounced insulin resistance and type 2 diabetes.

Insulin resistance in the AR10KO mouse likely results from reduced glucose flux into adipose because the WAT

transcriptional profiles are similar in the AR10KO and adipose GLUT4 KO models, two different models of reduced insulin-stimulated glucose transport into adipocytes. Rab10, in addition to its role in GLUT4 trafficking, functions in the control of a number of transport processes delivering proteins to the plasma membrane. Of particular interest is the proposed role of Rab10 in the control of endoplasmic reticulum (ER) morphology (45) because the perturbation of ER function downstream of Rab10 deletion could have functional consequences on adipocyte biology beyond insulin regulation of GLUT4 trafficking. The observations that Rab10 KO adipocytes develop normally and that the levels of circulating leptin and adiponectin, two major adipokines, are unchanged in AR10KO mice suggest that the ER function is not grossly altered by Rab10 KO. The gene set enrichment analyses between the AR10KO and adipose GLUT4 KO WAT shows that the WAT transcriptomes, which may cumulatively mediate the in vivo phenotypes, are similarly altered, strongly supporting reduced insulin-stimulated glucose transport in mediating whole-body insulin resistance in AR10KO mice, as seen with KO of adipose GLUT4 (7). Transcription of three of four mediators of the adipose GLUT4 KO metabolic phenotype, Bckdhb, ChREBP, and Nnmt, were significantly altered in the AR10KO mice. These data reinforce the proposal that reduced adipose glucose uptake in AR10KO mice contributes to the metabolic phenotype. However, it should be noted that the phenotypes of the KO models are not identical in that they have differences in levels of whole-body glucose uptake, muscle glucose uptake, and suppression of hepatic glucose production during euglycemic-hyperinsulinemic clamp. Possible explanations include differences in genetic background, the cre promoter used to target adipose, mouse housing facilities, as well as compensation induced in the adipose GLUT4 KO, where all insulin-stimulated glucose uptake is lost.

Insulin resistance in the AR10KO model, which is characterized by an aberrant ITT result as well as reduced glucose infusion rate during euglycemic-hyperinsulinemic clamp, establishes the physiological relevance of Rab10 in adipose insulin action. The alteration in GLUT4 trafficking produces insulin resistance without overt changes in glucose tolerance or fasting blood glucose level, a phenotype that is similar to human physiology during the early stages of insulin resistance, where hyperinsulinemia allows for normal glucose tolerance. Although trends are observed for decreased whole-body and muscle glucose uptake during clamp, the magnitude of these changes is minor compared with the striking hepatic insulin resistance. This demonstrates a clear axis between adipose insulin-stimulated glucose uptake and liver insulin sensitivity. Because the inhibition of insulin action on adipocyte GLUT4 translocation is incomplete, the AR10KO phenotype highlights that a fully functional adipocyte glucose uptake response to insulin is vital for the maintenance of whole-body insulin sensitivity.

During the euglycemic-hyperinsulinemic clamp, insulin suppression of plasma free fatty acid levels is intact. Furthermore, the in vivo defect in adipose glucose uptake was ~50%, reflecting the expected defect due to the loss of Rab10, without additional inhibition that might be expected from adipose insulin resistance. This suggests that adipose insulin sensitivity is unimpaired. These observations strongly support the notion that adipocytes use insulin-stimulated glucose uptake directly to sense the whole-body metabolic state and to modulate liver insulin sensitivity accordingly.

In conclusion, the AR10KO mouse demonstrates that Rab10 is essential for the full effect of insulin on GLUT4 translocation, emphasizes the significance of a full description of insulin regulation of GLUT4 trafficking, and highlights that even partial reductions of glucose flux into adipose severely impairs hepatic insulin sensitivity, producing systemic insulin resistance.

References

1. Holman GD, Lo Leggio L, Cushman SW. Insulin-stimulated GLUT4 glucose transporter recycling. A problem in membrane protein subcellular trafficking through multiple pools. J Biol Chem 1994;269:17516–17524
2. Yeh JI, Verhey KJ, Birnbaum MJ. Kinetic analysis of glucose transporter trafficking in fibroblasts and adipocytes. Biochemistry 1995;34:15523–15531
3. Karylowski O, Zeigerer A, Cohen A, McGraw TE. GLUT4 is retained by an intracellular cycle of vesicle formation and fusion with endosomes. Mol Biol Cell 2004;15:870–882

4.   Cushman SW, Wardzala LJ. Potential mechanism of insulin action on glucose transport in the isolated rat adipose cell. Apparent translocation of intracellular transport systems to the plasma membrane. J Biol Chem 1980;255:4758–4762

5.   Suzuki K, Kono T. Evidence that insulin causes translocation of glucose transport activity to the plasma membrane from an intracellular storage site. Proc Natl Acad Sci U S A 1980;77:2542–2545

6.   Zisman A, Peroni OD, Abel ED, et al. Targeted disruption of the glucose transporter 4 selectively in muscle causes insulin resistance and glucose intolerance. Nat Med 2000;6:924–928

7.   Abel ED, Peroni O, Kim JK, et al. Adipose-selective targeting of the GLUT4 gene impairs insulin action in muscle and liver. Nature 2001;409:729–733

8.   Lizunov VA, Lee JP, Skarulis MC, Zimmerberg J, Cushman SW, Stenkula KG. Impaired tethering and fusion of GLUT4 vesicles in insulin-resistant human adipose cells. Diabetes 2013;62:3114–3119

9.   Zierath JR, Houseknecht KL, Gnudi L, Kahn BB. High-fat feeding impairs insulin-stimulated GLUT4 recruitment via an early insulin-signaling defect. Diabetes 1997;46:215–223

10.   Maianu L, Keller SR, Garvey WT. Adipocytes exhibit abnormal subcellular distribution and translocation of vesicles containing glucose transporter 4 and insulin-regulated aminopeptidase in type 2 diabetes mellitus: implications regarding defects in vesicle trafficking. J Clin Endocrinol Metab 2001;86:5450–5456

11.   Eguez L, Lee A, Chavez JA, et al. Full intracellular retention of GLUT4 requires AS160 Rab GTPase activating protein. Cell Metab 2005;2:263–272

12.   Sano H, Kane S, Sano E, et al. Insulin-stimulated phosphorylation of a Rab GTPase-activating protein regulates GLUT4 translocation. J Biol Chem 2003;278:14599–14602

13.   Sano H, Eguez L, Teruel MN, et al. Rab10, a target of the AS160 Rab GAP, is required for insulin-stimulated translocation of GLUT4 to the adipocyte plasma membrane. Cell Metab 2007;5:293–303

14.   Larance M, Ramm G, Stöckli J, et al. Characterization of the role of the Rab GTPase-activating protein AS160 in insulin-regulated GLUT4 trafficking. J Biol Chem 2005;280:37803–37813

15.   Chen Y, Wang Y, Zhang J, et al. Rab10 and myosin-Va mediate insulin-stimulated GLUT4 storage vesicle translocation in adipocytes. J Cell Biol 2012;198:545–560

16.   Kane S, Sano H, Liu SC, et al. A method to identify serine kinase substrates. Akt phosphorylates a novel adipocyte protein with a Rab GTPase-activating protein (GAP) domain. J Biol Chem 2002;277:22115–22118

17.   Mîinea CP, Sano H, Kane S, et al. AS160, the Akt substrate regulating GLUT4 translocation, has a functional Rab GTPase-activating protein domain. Biochem J 2005;391:87–93

18.   Perret P, Ghezzi C, Ogier L, et al. Biological studies of radiolabeled glucose analogues iodinated in positions 3, 4 or 6. Nucl Med Biol 2004;31:241–250

19.   Camporez JP, Jornayvaz FR, Lee HY, et al. Cellular mechanism by which estradiol protects female ovariectomized mice from high-fat diet-induced hepatic and muscle insulin resistance. Endocrinology 2013;154:1021–1028

20.   Dobin A, Davis CA, Schlesinger F, et al. STAR: ultrafast universal RNA-seq aligner. Bioinformatics 2013;29:15–21

21.   Anders S, Pyl PT, Huber W. HTSeq—a Python framework to work with high-throughput sequencing data. Bioinformatics 2015;31:166–169

22.   Trapnell C, Williams BA, Pertea G, et al. Transcript assembly and quantification by RNA-Seq reveals unannotated transcripts and isoform switching during cell differentiation. Nat Biotechnol 2010;28:511–515

23.   Ritchie ME, Phipson B, Wu D, et al. limma powers differential expression analyses for RNA-sequencing and microarray studies. Nucleic Acids Res 2015;43:e47

24.   Subramanian A, Tamayo P, Mootha VK, et al. Gene set enrichment analysis: a knowledge-based approach for interpreting genome-wide expression profiles. Proc Natl Acad Sci U S A 2005;102:15545–15550

25.   Eguchi J, Wang X, Yu S, et al. Transcriptional control of adipose lipid handling by IRF4. Cell Metab 2011;13:249–259

26.   Lv P, Sheng Y, Zhao Z, et al. Targeted disruption of Rab10 causes early embryonic lethality. Protein Cell 2015;6:463–467

27.   Randhawa VK, Ishikura S, Talior-Volodarsky I, et al. GLUT4 vesicle recruitment and fusion are differentially regulated by Rac, AS160, and Rab8A in muscle cells. J Biol Chem 2008;283:27208–27219

28.   Dawson K, Aviles-Hernandez A, Cushman SW, Malide D. Insulin-regulated trafficking of dual-labeled glucose transporter 4 in primary rat adipose cells. Biochem Biophys Res Commun 2001;287:445–454

29.   Lampson MA, Schmoranzer J, Zeigerer A, Simon SM, McGraw TE. Insulin-regulated release from the endosomal recycling compartment is regulated by budding of specialized vesicles. Mol Biol Cell 2001;12:3489–3501

30.   Zeigerer A, Lampson MA, Karylowski O, et al. GLUT4 retention in adipocytes requires two intracellular insulin-regulated transport steps. Mol Biol Cell 2002;13:2421–2435

31.   Greenberg AS, Egan JJ, Wek SA, Garty NB, Blanchette-Mackie EJ, Londos C. Perilipin, a major hormonally regulated adipocyte-specific phosphoprotein associated with the periphery of lipid storage droplets. J Biol Chem 1991;266:11341–11346

32.   Scherer PE, Williams S, Fogliano M, Baldini G, Lodish HF. A novel serum protein similar to C1q, produced exclusively in adipocytes. J Biol Chem 1995;270:26746–26749

33.   Chavez JA, Roach WG, Keller SR, Lane WS, Lienhard GE. Inhibition of GLUT4 translocation by Tbc1d1, a Rab GTPase-activating protein abundant in skeletal muscle, is partially relieved by AMP-activated protein kinase activation. J Biol Chem 2008;283:9187–9195

34.   Huang G, Buckler-Pena D, Nauta T, et al. Insulin responsiveness of glucose transporter 4 in 3T3-L1 cells depends on the presence of sortilin. Mol Biol Cell 2013;24:3115–3122

35.   Sivitz WI, Walsh SA, Morgan DA, Thomas MJ, Haynes WG. Effects of leptin on insulin sensitivity in normal rats. Endocrinology 1997;138:3395–3401

36.   Berg AH, Combs TP, Du X, Brownlee M, Scherer PE. The adipocyte-secreted protein Acrp30 enhances hepatic insulin action. Nat Med 2001;7:947–953

37.   Yang Q, Graham TE, Mody N, et al. Serum retinol binding protein 4 contributes to insulin resistance in obesity and type 2 diabetes. Nature 2005;436:356–362

38.   Herman MA, Peroni OD, Villoria J, et al. A novel ChREBP isoform in adipose tissue regulates systemic glucose metabolism. Nature 2012;484:333–338

39.   Herman MA, She P, Peroni OD, Lynch CJ, Kahn BB. Adipose tissue branched chain amino acid (BCAA) metabolism modulates circulating BCAA levels. J Biol Chem 2010;285:11348–11356

40.   Kraus D, Yang Q, Kong D, et al. Nicotinamide N-methyltransferase knockdown protects against diet-induced obesity. Nature 2014;508:258–262

41.   Jedrychowski MP, Gartner CA, Gygi SP, et al. Proteomic analysis of GLUT4 storage vesicles reveals LRP1 to be an important vesicle component and target of insulin signaling. J Biol Chem 2010;285:104–114

42.   Wang D, Lou J, Ouyang C, et al. Ras-related protein Rab10 facilitates TLR4 signaling by promoting replenishment of TLR4 onto the plasma membrane. Proc Natl Acad Sci U S A 2010;107:13806–13811

43.   Lerner DW, McCoy D, Isabella AJ, et al. A Rab10-dependent mechanism for polarized basement membrane secretion during organ morphogenesis. Dev Cell 2013;24:159–168

44.   Liu Y, Xu XH, Chen Q, et al. Myosin Vb controls biogenesis of post-Golgi Rab10 carriers during axon development. Nat Commun 2013;4:2005

45.   English AR, Voeltz GK. Rab10 GTPase regulates ER dynamics and morphology. Nat Cell Biol 2013;15:169–178

46.   Lansey MN, Walker NN, Hargett SR, Stevens JR, Keller SR. Deletion of Rab GAP AS160 modifies glucose uptake and GLUT4 translocation in primary skeletal muscles and adipocytes and impairs glucose homeostasis. Am J Physiol Endocrinol Metab 2012;303:E1273–E1286

47.   Wang HY, Ducommun S, Quan C, et al. AS160 deficiency causes whole-body insulin resistance via composite effects in multiple tissues. Biochem J 2013;449:479–489

48.   Quan C, Xie B, Wang HY, Chen S. PKB-Mediated Thr649 Phosphorylation of AS160/TBC1D4 Regulates the R-Wave Amplitude in the Heart. PLoS One 2015; 10:e0124491

49.   Alves DS, Thulin G, Loffing J, Kashgarian M, Caplan MJ. Akt substrate of 160 kD regulates Na+,K+-ATPase trafficking in response to energy depletion and renal ischemia. J Am Soc Nephrol 2015;26:2765–2776

50.   Zeigerer A, McBrayer MK, McGraw TE. Insulin stimulation of GLUT4 exo-cytosis, but not its inhibition of endocytosis, is dependent on RabGAP AS160. Mol Biol Cell 2004;15:4406–4415

51.   Koumanov F, Pereira VJ, Richardson JD, Sargent SL, Fazakerley DJ, Holman GD. Insulin regulates Rab3-Noc2 complex dissociation to promote GLUT4 translocation in rat adipocytes. Diabetologia 2015;58:1877–1886

52.   Yu C, Cresswell J, Löffler MG, Bogan JS. The glucose transporter 4-regulating protein TUG is essential for highly insulin-responsive glucose uptake in 3T3-L1 adipocytes. J Biol Chem 2007;282:7710–7722